Trans Indian Inst Met (2022) 75(9):2241–2253
https://doi.org/10.1007/s12666-022-02589-3

ORIGINAL ARTICLE

Production of MWCNT-Reinforced Aluminum Foams Via Powder Space-Holder Technique and Investigation of their Mechanical Properties

Abdullatif Emar Salem Abo sbia[1] · Arif Uzun[2]

Received: 7 September 2021 / Accepted: 11 March 2022 / Published online: 16 April 2022

Abstract In this study, aluminum foams reinforced with multi-walled carbon nanotubes (0%, 0.5%, 1%, and 2% by weight) were produced by powder metallurgy method using different proportions of spherical urea (15%, 30%, and 50% by weight) as space holder. It analyzes the pore morphology and pore distribution of the produced composite foams and examines their mechanical properties under qua-static compressive loading. The results show that the effect of multi-walled carbon nanotubes existing in the cell wall on pore morphology and pore distribution was insignificant. The highest hardness value (65 HV) was determined in the foam samples containing 2% multi-walled carbon nanotube produced with 15% urea. Composite aluminum foam samples with 30–69% porosity and 0.84–1.90 g cm^{-3} density were successfully produced. The compression properties of the samples decreased with the decrease in the relative densities.

Keywords Aluminum foam · Composite · Energy absorption · Multi-walled carbon nanotubes (MWCNT) · Mechanical properties · Urea

✉ Arif Uzun
auzun@kastamonu.edu.tr

[1] Department of Materials Science and Engineering, Institute of Science, Kastamonu University, Kastamonu, Turkey

[2] Department of Mechanical Engineering, Kastamonu University, Kastamonu, Turkey

1 Introduction

Metallic foams have attracted much attention from researchers due to their lightness, high impact energy absorption, vibration, and sound attenuation [1]. Generally, based on the preparation methods of metallic foams, they are divided into two categories: closed cell and open cell. Powder metallurgy and melting foaming methods are widely used for closed-cell foams, while powder space-holder and chemical vapor dissolution (CVD) methods are widely preferred for open-cell foams. The space-holder method is one of the most important techniques because it allows parameters such as porosity ratio and pore morphology (pore shape and size) of metallic foams to be easily controlled [2–4]. The mechanical properties of the metallic foam depend on the cell morphology, cell wall thickness, and properties of the base materials [5]. In particular, the energy absorption performance of the foams is related to the failure modes of the cells [6]. During deformation, these modes generally occur as tearing, twisting, or buckling of cell walls [6–8]. In the previous literature, it has been stated that aluminum foams exhibit three typical phases under compression stresses. These are linear elastic region ($\varepsilon < 0.05$), plateau region ($0.05 < \varepsilon < 0.5$), and densification region ($\varepsilon > 0.5$). The width of the plateau area shows the magnitude of the energy absorption capacity. Energy absorption capacity increases as this region expands [9]. The mechanical properties of aluminum foams can be improved by adding alloy elements or reinforcements. For example, aluminum foams' compression strength, plateau stress, and energy absorption capacity increase with the addition of alloy elements, such as Mn, Ni, or Sc, to aluminum foam [10, 11]. Studies on aluminum composite foams reinforced with microscale reinforcing elements have also increased

[12–15]. The mechanical properties of these composite foams are improved compared to pure aluminum due to the high stiffness of the reinforcing element [12]. However, possible weak bonding at the interface between the reinforcing element and the Al matrix can cause the foams to exhibit brittle deformation behavior and limited energy absorption capacity [12, 16, 17].

Carbon nanotubes (CNTs) can be considered as the perfect reinforcing element for many metallic composite foams due to their lightweight and high strength [4, 12, 18–20]. The compression strength of composite foams reinforced with CNTs is generally reported to be higher than that of non-reinforced aluminum foams [21]. Compared to composite foams with reinforcing elements, such as Al_2O_3 and SiC, CNTs relatively reduce the plasticity of composite foams [18, 22, 23]. Failure to distribute CNTs homogeneously in the structure is a common difficulty in composite production. In this regard, a new method that combines colloidal processing-powder technology [24], high-energy ball milling methods [25, 26], and flake powder metallurgy [27] are proposed by researchers. Duarte et al. [28, 29] tried a new method by combining colloidal process and powder technology to achieve a good distribution of CNTs in the Al matrix and a complementary structure. Al–12Si alloy foams were reinforced using MWCTs–COOH solution in their study. Yang et al. [3] used CVD/shock time ball milling/space-holder methods to produce composite foams containing homogeneously distributed CNT. Researchers observed that the yield stress was about three times higher in foams reinforced with 2, 2.5, and 3 wt% CNTs compared to non-reinforced foams. Further, Yadav et al. [30] produced LM13-SiC/MWCNT hybrid composite foams using the melt-stirring method and determined their high-temperature behavior at different strain rates. Their results showed that when SiC and CNTs are added to the aluminum matrix, the alloy is restricted as plastic due to the resistance against the dislocation movement. In addition, Aldoshan and Khanna [21] stated that mechanical properties improve with an increase in the relative density of the 2 wt.% CNT-reinforced AA5083 foams produced by liquid metallurgy. Zhang et al. [25] studied the compression and energy absorption properties of closed-cell aluminum foams with different CNT contents (0, 0.2, 0.5, 0.8 wt%) produced by the modified melt foaming method. According to their results, the maximum compression property is obtained in composite foams reinforced with 0.5 wt.% CNTs. They also achieved 43% higher yield stress than CNT-free foams. Many different Al alloys were used in most of these studies, such as pure Al, Al–12Si, AA5083, and LM13. In addition, CNTs are reinforced to aluminum foams using different methods. For example, melt-stirring processes, CVD/ball milling/space holder, colloidal process/powder metallurgy, and modified melt foaming.

It is seen that this research mainly focuses on the effect of CNT on the properties of light aluminum foams with more than 60% porosity. Our study produces MWCNT/Al foams with different porosity and CNT contents using different amounts of urea (10, 30, and 50 wt%) using the space-holder method. In particular, the dispersion mode and effect of CNTs on the mechanical properties of high-density aluminum foams are unclear and need further study. To date, almost no research has been reported on closed-cell high-density aluminum foams containing CNTs prepared by the spacer method. Therefore, the current study mainly focuses on determining the effect of MWCNTs on the mechanical properties of high-density closed-cell aluminum foam.

2 Experimental Procedures

2.1 Materials

In the experimental studies, Al powder from Ecka Granule company as matrix material (99.5% purity— < 44 μm in size) and multi-walled carbon nanotubes from Cheap Tubes company as the reinforcing element (MWCNT-mean external diameter > 50 nm, length is 10–20 μm) were obtained. Besides, spherical-shaped urea (CH_4N_2O) with an average diameter of 1.5 mm was used in order to form pores in the structure. Figure 1 shows scanning electron microscope images of the powders and photographs of spherical-shaped urea.

2.2 Production of MWCNT/Al Composite Foams

Mixing operations were started primarily with starting powders. For this process, MWCNT particles (0, 0.5, 1, and 2%) were added to the aluminum powders separately and mixed at 400 rpm for 60 min in the planetary ball mill (Retsch PM100). In order for the ball/powder rate to be 5:1 by weight, stainless steel balls with 8-mm diameter were added into the mixture powder. One percent stearic acid was added into the mixture to ensure effective distribution of MWCNTs, prevent the powders from adhering to container walls and balls, and minimize the cold-welding effect of the powder particles. After the MWCNT/Al mixing process was completed, the second mixing process was started. In this process, urea granules (15, 30, and 50%) were added into the MWCNT/Al mixture. Before the mixing process, ethanol was sprayed to the urea granules in order to obtain an adhesive surface with adhesion of MWCNT/Al mixture powders. Thus, homogeneous distribution of the powders on the urea granules was provided.

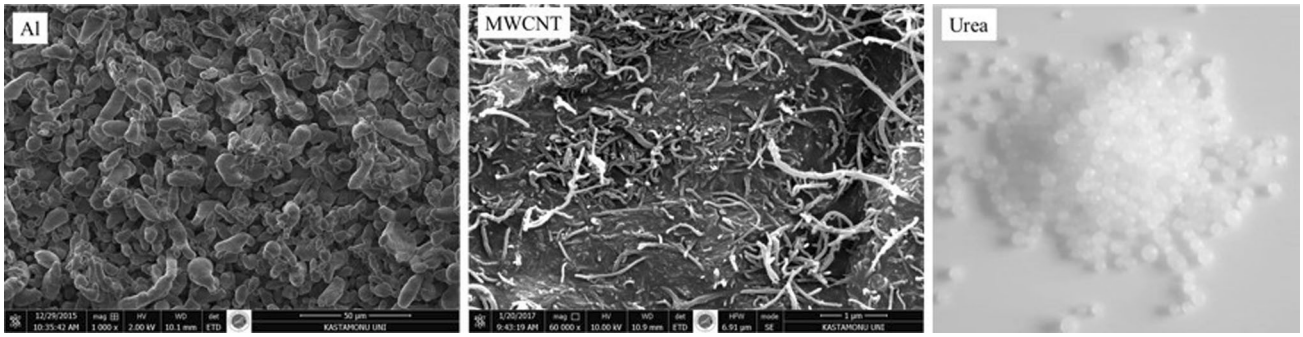

Fig. 1 Scanning electron microscope images of the powders and photograph of spherical-shaped urea

The prepared metallic powder/urea mixture was stirred for two hours on a rotary mixer and made ready for the compression process. The prepared powders were unidirectionally compressed in a steel mold under 600 MPa pressure with the help of a hydraulic press with a compressive capacity of 120 tons. After the compression, cylindrical samples with a diameter of 27 mm were produced. In order to dissolve and remove urea from the compact samples after compression, the samples were kept at water bath at 80 °C for 3 h. They were dried at 60 °C after washing the samples with ethanol [31]. The obtained foams were subjected to sintering process at 650 °C for 2 h. The fabrication process of MWCNT/Al composite foams is illustrated in Fig. 2.

2.3 Characterization

2.3.1 Macro- and Microstructural Analysis

The produced composite foams were cut from middle with a wire cutting machine for micro- and macrostructural analysis. The samples were then sanded with 120, 280, 320, 600, 800, 1200, 1500, and 2000 mesh SiC sandpapers and polished with a diamond solution in accordance with

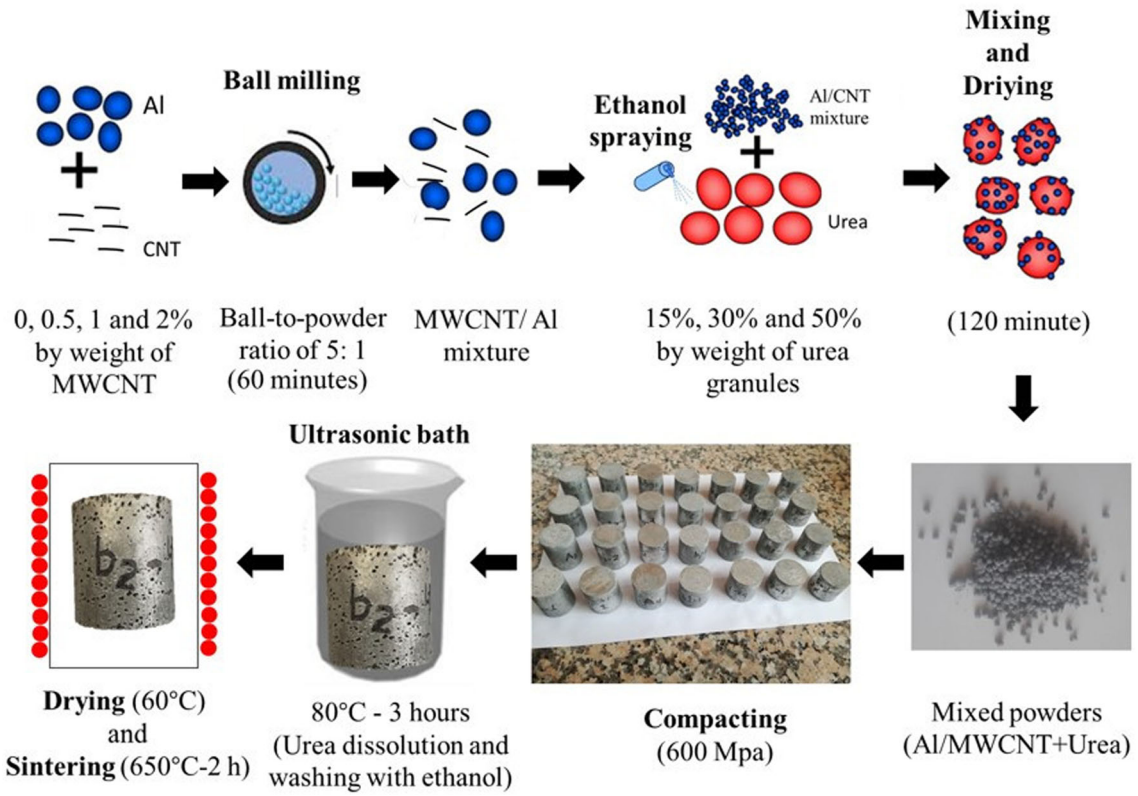

Fig. 2 The production process of MWCNT/Al composite foams

the standard metallographic procedure. Thus, the samples were made ready for macroporosity and microstructural analysis. In microstructure examinations, FEI brand Quanta FEG 250 model scanning electron microscope (SEM) including energy-dispersive spectrometry (EDS) was used.

2.3.2 Density Measurement

Due to the dimensional size, the densities of the produced samples (ρ_S) were calculated based on the weight (m_h) to volume (v) ratio of the samples in air by using the formula given in Eq. 1.

$$\rho s = \frac{\mathrm{mh}}{v}. \tag{1}$$

The theoretical densities (ρ_T) of the composite foams were calculated based on the mixing rule. Accordingly, the weight percentage rate ($\%W_x$) of each component forming the sample was multiplied with their densities (ρ_x) and the theoretical density was calculated by summing the obtained values (Eq. 2).

$$\rho_T = [(\%W_1) \times \rho_1] + [(\%W_2) \times \rho_{12}] + \cdots + [(\%W_n) \times \rho_s]. \tag{2}$$

The relative density (ρ^*) values were obtained by the ratio of the actual density to the theoretical density (Eq. 3).

$$\rho* = {}^{\rho_s}/_{\rho_T} \tag{3}$$

The porosity ratio (P) of the obtained foam samples was calculated with the formula given in Eq. 4.

$$P = (1 - \left({}^{\rho_s}/_{\rho_T}\right) X100. \tag{4}$$

2.3.3 Compression Test

In order to determine the crushing behaviors of the produced composite foams, compression tests were conducted at the deformation rate of 1 mm min^{-1}. For these tests, Shimadzu brand Autograph AGS-X model universal test device was used. Energy absorption (E) was obtained by calculating the area under the strain–stress curves obtained after the compression test. This can be expressed as in Eq. 5.

$$E = \int_0^{\varepsilon} \sigma d\varepsilon. \tag{5}$$

The average stress in the range of ε: 0.2–0.4 strain is expressed with following relations, as mentioned in Eq. (6).

$$\sigma_{avr} = \frac{\int_{\varepsilon_{0.2}}^{\varepsilon_{0.4}} \sigma d\varepsilon}{\varepsilon_{0.4} - \varepsilon_{0.2}}. \tag{6}$$

2.3.4 Microhardness

The hardness measurements were conducted using Shimadzu (HMV-G) microhardness device. The hardness measurements of the produced composite foams were conducted by applying 100 g load from the prepared cell wall cross sections [32–34]. The microhardness values were evaluated by taking mean of minimum five measurements for each sample.

3 Results and Discussion

3.1 Morphological Study

The cross sections of MWCNT/Al composite foams are presented in Fig. 3. It was observed that a large number of pores spread throughout the cross section of the foams with an increasing amount of urea. The pores of MWCNT/Al composite foams with different sizes were relatively homogeneously dispersed in the structure, which took the shape of the original spherical urea granules. MWCNT/Al composite foams produced with different ratios of urea had fewer angular pores than foams produced with other spacers, such as NaCl [35]. The spherical pore structure can help reduce regional stress concentrations during deformation and increase the strength values of MWCNT/Al foams. Furthermore, structural properties, such as pore size and porosity ratio of the composite foams produced with urea used in the study, can be easily controlled [2, 36]. The spherical shape of the urea can enable the particles to move and rearrange easily during the compaction of the powders. It also contributes to homogeneous pore distribution by enabling particles to move and rearrange easily during the compaction of the powders. However, the effect of the added MWCNT particles on the macroscale pore structure is not much. It was found that the pore size of composite foams did not change depending on the content of MWCNT (Table 1).

The influence of urea on the physical properties, such as density, pore size, porosity, and relative density of composite foams, was quite strong compared to MWCNT particles. As expected, a significant increase was observed in the values obtained depending on the amount of urea, independent of the MWCNT content (Fig. 4). Results showed that the amount of MWCNT had no significant effect on the porosity ratio of the foams. The measured values were relatively higher than the proportional value of the amount of urea used. Accordingly, the average porosity rates in the MWCNT/Al composite foams produced with

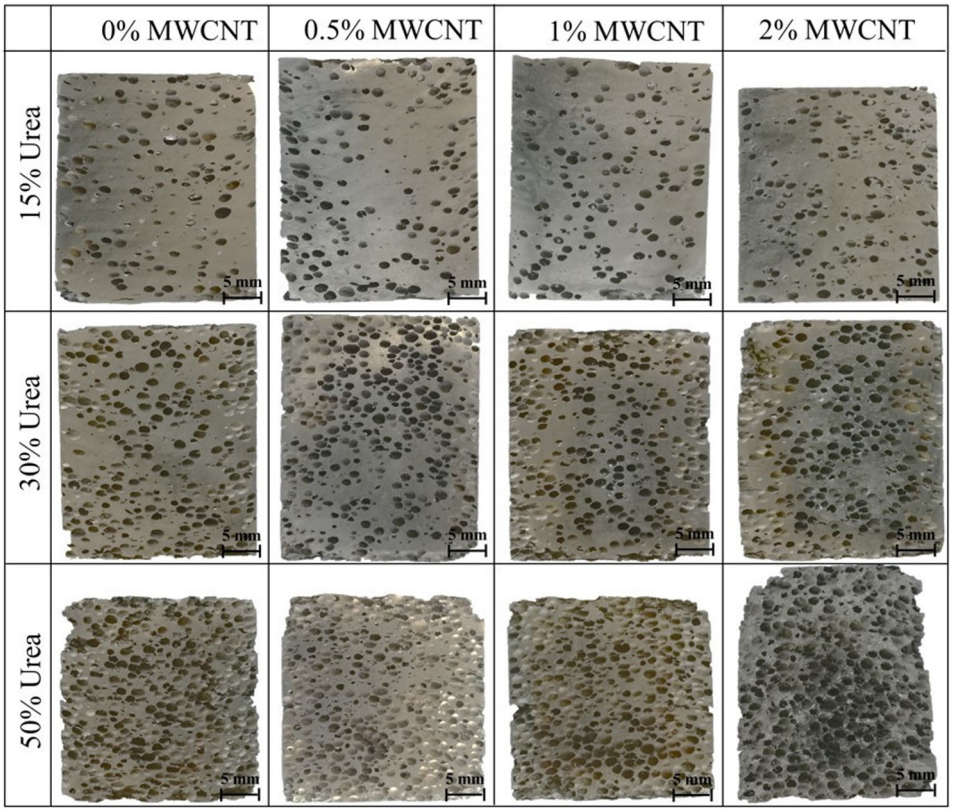

Fig. 3 Macrostructure images of aluminum foams with and without MWCNT

Table 1 Pore diameter, density, porosity, relative density, and microhardness of MWCNT/Al composite foams as a function of urea and MWCNT contents

Urea (wt.%)	MWCNT (wt.%)	Pore diameter (mm)	Density (g.cm^{-3})	Porosity (%)	Relative density	Microhardness (HV)
15	***0***	1.27 ± 0.23	1.97 ± 0.08	27.0 ± 3.12	0.73 ± 0.03	38.47 ± 2.32
	0.5	1.26 ± 0.28	1.88 ± 0.04	30.1 ± 1.53	0.70 ± 0.02	52.90 ± 1.91
	1	1.25 ± 0.14	1.84 ± 0.01	31.7 ± 0.54	0.68 ± 0.01	60.27 ± 2.71
	1.5	1.25 ± 0.19	1.91 ± 0.03	28.5 ± 1.23	0.71 ± 0.01	65.43 ± 2.70
30	***0***	1.32 ± 0.16	1.44 ± 0.03	46.8 ± 1.23	0.53 ± 0.01	38.67 ± 1.12
	0.5	1.35 ± 0.29	1.33 ± 0.03	50.5 ± 1.04	0.49 ± 0.01	35.07 ± 1.68
	1	1.28 ± 0.25	1.36 ± 0.05	49.5 ± 1.75	0.50 ± 0.02	42.03 ± 2.03
	1.5	1.29 ± 0.21	1.33 ± 0.05	50.3 ± 2.05	0.50 ± 0.02	57.70 ± 1.39
50	***0***	1.51 ± 0.44	0.89 ± 0.02	67.2 ± 0.71	0.33 ± 0.01	39.93 ± 1.72
	0.5	1.45 ± 0.71	0.88 ± 0.03	67.4 ± 1.26	0.33 ± 0.01	41.07 ± 1.66
	1	1.45 ± 0.44	0.82 ± 0.03	69.4 ± 1.00	0.31 ± 0.01	40.77 ± 2.01
	1.5	1.43 ± 0.36	0.77 ± 0.05	71.4 ± 1.79	0.29 ± 0.01	54.97 ± 1.31

15%, 30%, and 50% urea were obtained as 29.58 ± 2.04%, 49.40 ± 1.72%, and 68.97 ± 1.98%, respectively. The porosity of the MWCNT/Al composite foam was almost equal to the volume fraction of urea used. When calculated in volumetric ratios, the amounts of urea for foams produced with 15%, 30%, and 50% urea were approximately 26%, 47%, and 67%, respectively. This difference is mainly related to the presence of microspores between the compressed aluminum particles. Controlling the total porosity and pore size distribution in a porous structure plays a key role for materials adapted for specific applications [37]. Figure 5 shows the densities of MWCNT/Al composite foams. As is known, the density change in metallic foams is directly related to the porosity ratio. As

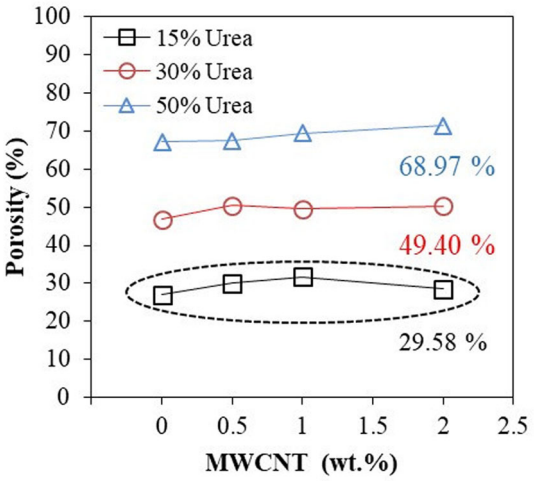

Fig. 4 Porosity ratios of MWCNT/Al composite foams

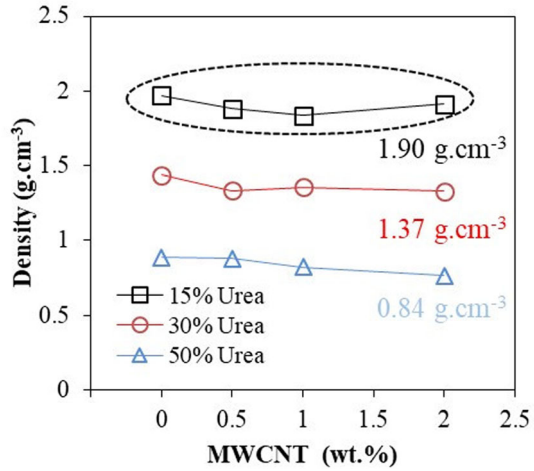

Fig. 5 Density values of MWCNT/Al composite foams

the porosity increased in the structure, the density values decreased. The mean density values of the MWCNT/Al foams produced with 15%, 30%, and 50% urea were 1.90 ± 0.05 g cm^{-3}, 1.37 ± 0.04 g cm^{-3}, and 0.84 ± 0.05 g cm^{-3}, respectively. According to these results, there was a proportional difference of approximately 44% between the maximum and minimum results. This difference was obtained with the change in the amount of urea at the rate of 35%.

Figure 6 shows the SEM images taken over the cell walls of the MWCNT/Al composite foams produced with 15% urea. Zhang et al. [25] stated that MWCNT particles were found in the cell wall in three forms for the foam structure containing 0.5% MWCNT. These forms were defined as being completely embedded in the cell wall, with both ends completely embedded and relatively located on the cell wall surface and completely located on the cell wall surface. In our study, one end of the MWCNTs was embedded in the cell wall, while the other end was relatively free. Additionally, MWCNTs identified by energy-dispersive X-ray spectroscopy (EDS) were found in the cell walls as tubular and sometimes agglomerated. It was observed that the agglomerated MWCNTs present on the aluminum powders could not be adequately dispersed during the mixing process. On the other hand, it has been reported that CNTs are almost evenly distributed on the surface of flaky Al powders due to the mechanical cutting effect of ball milling [38]. As observed from this figure at point 1, the analysis gave a mixture of 40%Al–50%C–10%O. The presence of oxygen might have resulted from the oxidation of aluminum during sample preparation, as it can be easily oxidized.

3.2 Cell Wall Microhardness

Figure 7 shows the average Vickers hardness value measured from the cell walls of MWCNT/Al composite foams, and the results are also given in Table 1. It is noted from the table that the values of microhardness increased with the addition of MWCNT. The measured Vickers hardness values were among 40–65 HV for MWCNT-reinforced aluminum foams, and the average hardness value of common aluminum foam fabricated by the conventional method only reached 30.3–34.7 HV [39]. The maximum hardness value (65 ± 3.70 HV) was obtained in the 2% MWCNT-reinforced foam sample produced with 15% urea. The hardness value in the foam samples without MWCNT produced with 15% urea was 39 ± 2.32 HV. With the addition of MWCNT, a hardness increase of approximately 66% was observed in the cell walls of the foam samples. The maximum hardness values of the samples produced with 30% and 50% urea were obtained with 2% MWCNT reinforcement. The hardness values obtained for both samples were 58 ± 1.39 HV and 55 ± 1.31 HV, respectively. Furthermore, the hardness values of the cell walls of the foams produced with a high amount of urea decreased due to microvoids formed in the cell walls. Similar results were also emphasized by Abhash et al. [40]. Also, in the study by Duarte et al. [24], a new approach modified by adding an advanced colloidal process step to the conventional powder metallurgy method to disperse MWCNTs was applied. The results of Vickers microhardness determined on the cell walls of foams with 0.5% CNT and without were 93.43 ± 19.30 HV and 60 HV $\pm$ 5.18 HV, respectively. Those results were considerably higher than our results.

3.3 Compressive Property

The deformation process (strain range of $\varepsilon = 0$–0.45) of MWCNT/Al foams during the quasi-static compression test

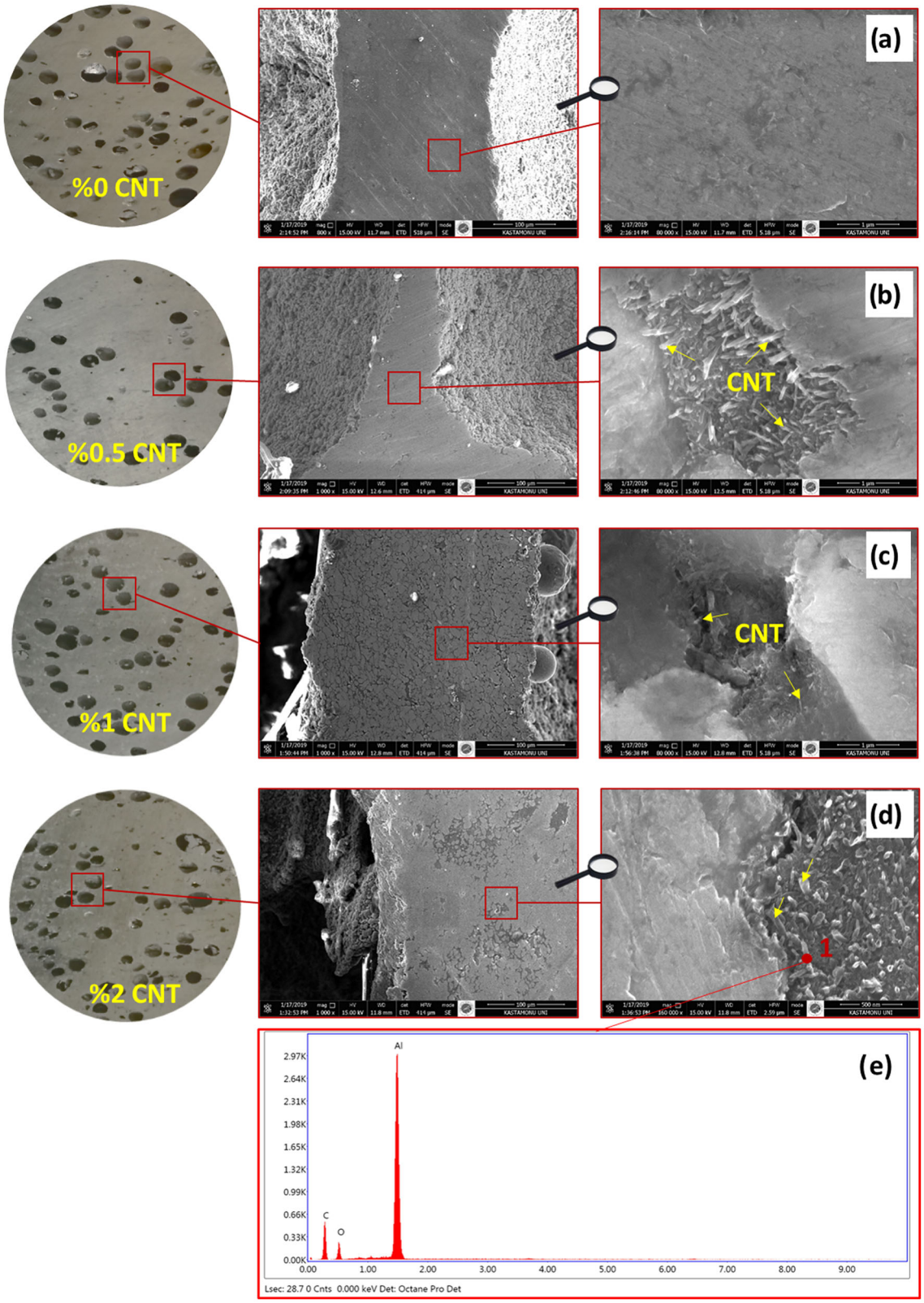

Fig. 6 SEM images of the cell walls of the MWCNT/Al composite foams; **a** 0% MWCNT, **b** 0.5% MWCNT, **c** 1% MWCNT, **d** 2% MWCNT, and **e** EDS result of point 1

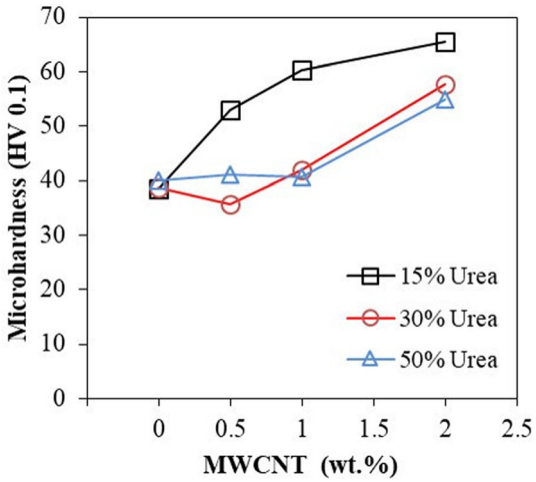

Fig. 7 Hardness values of the cell walls of MWCNT/Al composite foams

was recorded using a digital camera. Figures 8, 9, and 10 show the gradually crushing behaviors of MWCNT/Al foams during the compressive test. It could be seen that the samples began to deform on the lower or upper surfaces (strain < 0.15). Concentrated deformation in these regions led to the formation of many deformation bands. Although macro-sized samples had a relatively homogeneous pore structure, they showed inhomogeneous deformation behavior due to their structure under compression load. The general tendency was an increase in the fractures and breaks in the cell walls and outer surfaces of the samples, along with an increase in the amount of MWCNT [3, 4]. During compression, cell walls that moved toward each other resulted in friction, increasing the force required for compression. However, the strength of the foam decreased during the crushing or breaking of the cell walls [30]. As a result, deformation concentrated on weak cell walls and resulted in premature cell collapse. This contributed to an increase in the compression strain.

Figure 11 shows the stress–strain curves of the MWCNT/Al foams. The mean relative density values of the samples are also given on the graph. The curves of the foam samples was be divided into three regions: (i) the initial linear elastic region, (ii) the plateau region, and (iii) the densification region. The width (size) of the three regions varied depending on the relative density values and cell structures [41, 42]. The relative densities of the foam samples produced with 15% and 30% urea were very high. Therefore, there was a substantial strain hardening. In particular, the plateau region of the stress–strain curves of

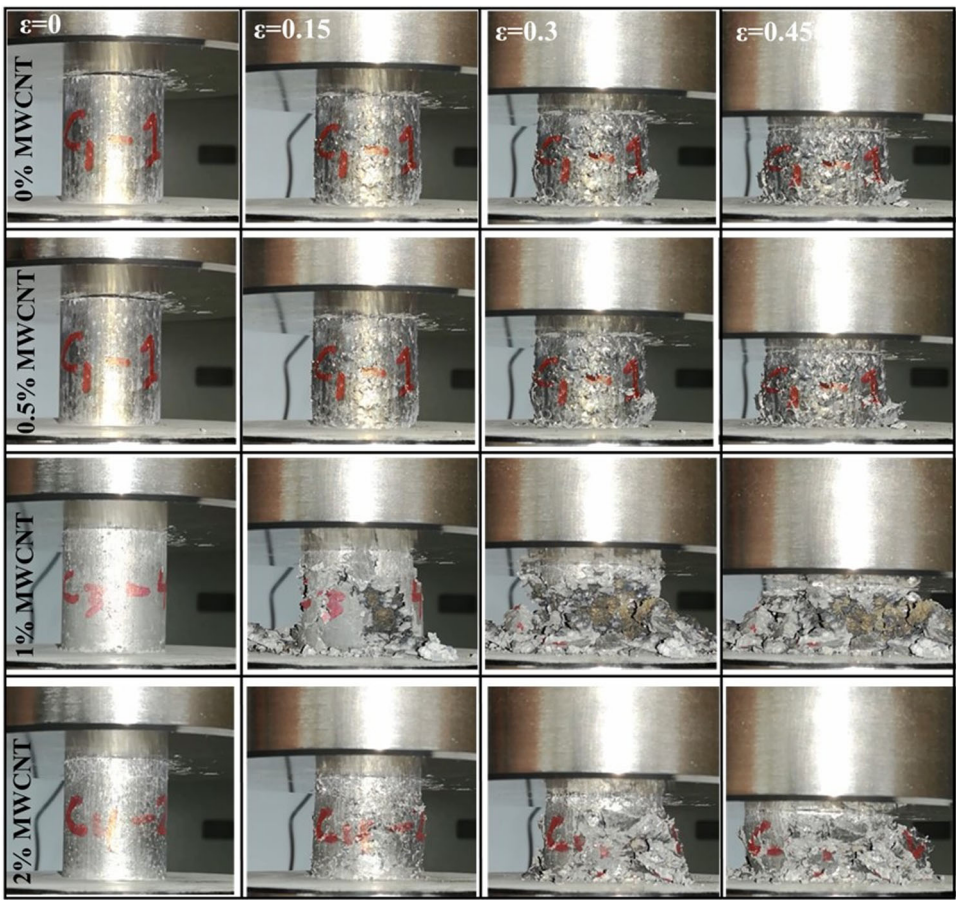

Fig. 8 Gradually crushing behaviors of MWCNT/Al composite foams produced with 15% urea

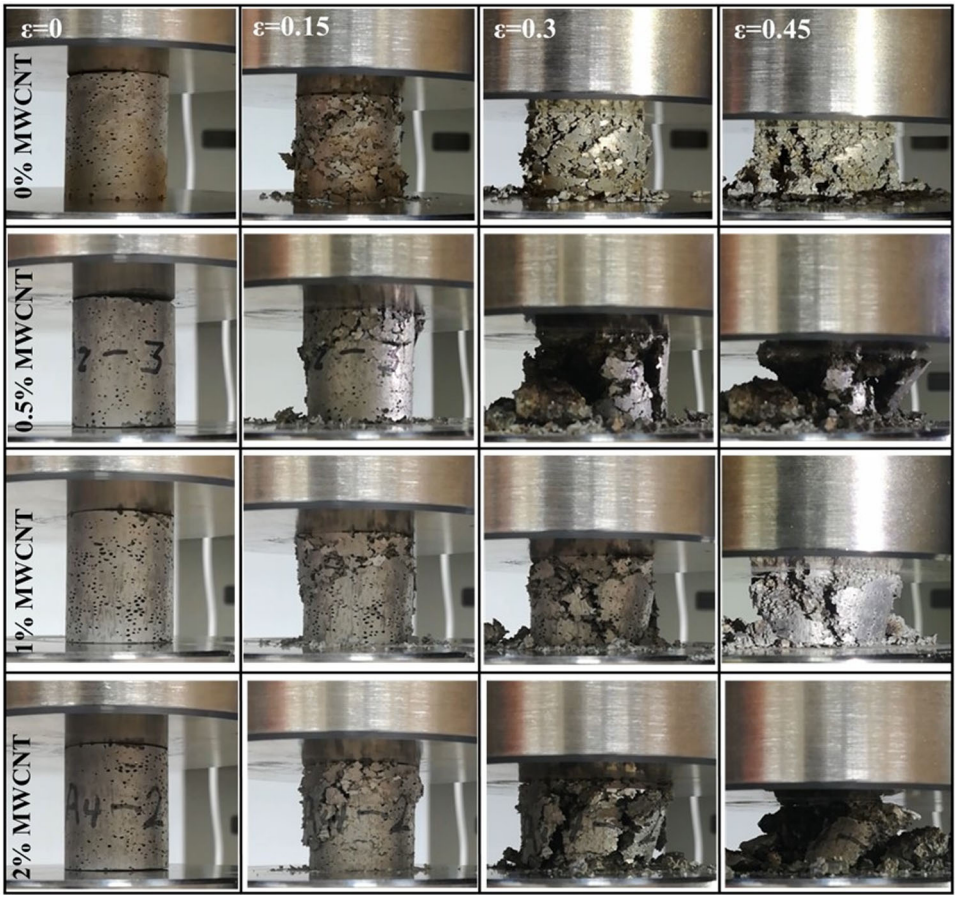

Fig. 9 Gradually crushing behaviors of MWCNT/Al composite foams produced with 30% urea

samples produced with 15% urea was not clearly defined. This region was much more sloped for high-density samples. It is clear that samples produced with 15% urea possessed more stiffness than others. Further, the curves of MWCNT-free samples were relatively smooth compared to others. This situation was caused by buckling of cell walls during deformation. On the other hand, some fluctuations occurred due to the breaking and collapse of pore walls, not buckling. These stress fluctuations were much smaller than aluminum foams reinforced with other ceramic phases [12, 13, 43, 44]. The space-holder technique ensured the correct control of aluminum foams' porosity and pore size. Thus, the effect of relative density on mechanical properties could be effectively investigated [45]. The compression properties decreased with the relative density of the foam as in other studies [45–48].

Figure 12 shows the variation of yield stress with urea and MWCNT. The maximum yield stress (57 MPa) was obtained in the 2% MWCNT-reinforced aluminum foam with a 0.71 relative density produced with 15% urea. In contrast, the minimum yield stress (3.4 MPa) was obtained in the 1% MWCNT-reinforced aluminum foam with a 0.31 relative density produced with 50% urea. The porosity ratios of both samples were calculated as 28.5% (2% MWCNT-reinforced aluminum foam produced with 15% urea) and 69.4% (1% MWCNT-reinforced aluminum foam produced with 50% urea). The solid phase is higher in volume in the samples produced with 15% urea. In this case, subjecting the cell wall to bending and twisting during the compression test resulted in a higher foam strength depending on the resistance of cell wall thickness [21]. The decrease in the relative density values in the samples produced with 50% urea caused thinning in the cell walls. In this case, the bending strength of the cell walls and the required inertia moments decreased, and the compression properties such as plastic collapse strength and average stress weakened [49].

According to the results, the effect of MWCNT particles on the initial yield stress had a complex correlation. An increase was observed in the yield stress of the foam samples produced with 15% urea, along with the increasing MWCNT rates. While the minimum yield stress was 36 MPa for the samples without MWCNT, the maximum yield stress (57 MPa) was obtained in the sample containing 2% MWCNT. According to this result, with the 2% change in MWCNT rate, an increase of 58.3% was obtained in the yield stress. This can be explained by the mechanism in which fiber reinforcement is relatively

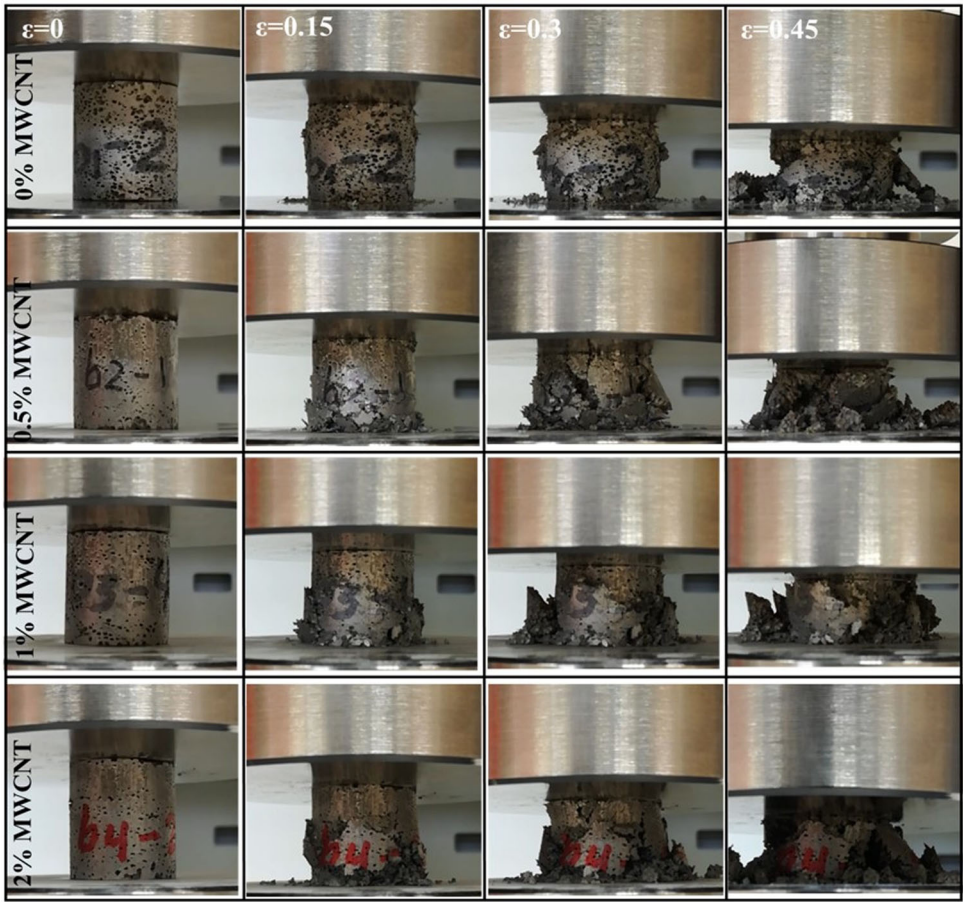

Fig. 10 Gradually crushing behaviors of MWCNT/Al composite foams produced with 50% urea

dominant, as in Al matrix composites reinforced with MWCNT [50–52]. Shear stresses corresponding to the applied force can be effectively transmitted from the matrix to MWCNTs [3]. On the other hand, a slight decrease occurred in the yield stress, while MWCNT rate in the foam samples produced with 30% and 50% urea increased. For foam samples produced with 30% urea, a minimum yield stress (14 MPa) was obtained with the addition of 2% MWCNT. The maximum yield stress (20 MPa) in these samples was obtained in the foam sample without MWCNT. According to the obtained data, there was a decrease of 30% in the yield stress. However, this decrease correlated with the MWCNT amount and the relative density of the samples. There was a similar trend in the foam samples produced with 50% urea. The MWCNTs found in the cell wall matrix did not generate a scatter-reinforcement effect sufficiently. Factors such as clustering of particles and weak interface binding are thought to cause this situation [30]. Usually, for cellular materials, the relative density is less than 0.3. The average stress in the range of ε: 0.2–0.4 strain was calculated rather than the plateau stresses, and it was found that the average stress of the foams decreased with MWCNT and urea as well as yield stress (Fig. 13).

3.4 Energy Absorption

Energy absorption curves determined by the integration of stress–strain curves are given in Fig. 14. The energy absorption capacity of samples with high relative density is significantly higher. These samples exhibit high strain hardening during compression, which can be attributed to the foam cell morphology and structural variables in terms of density [11, 12]. Structural variability initiates deformation when the pore density is at a maximum in the sample during compression. With the increasing stress, the deformation progresses toward the weak regions and the formation of more than one deformation band occur. As seen in the macroscopic pictures given in Fig. 3, the cell walls became thinner with the decrease in the relative density of the foam. The cell walls in these samples were broken or crushed more easily with the applied stress. Thus, lower plateau stresses and energy absorption properties were obtained.

Energy absorption curves for 0.3 strain are given in Fig. 15 to understand the effect of MWCNT on energy absorption and to compare samples with each other. It can be argued that MWCNTs weaken the energy absorption properties of pure aluminum foams for constant relative

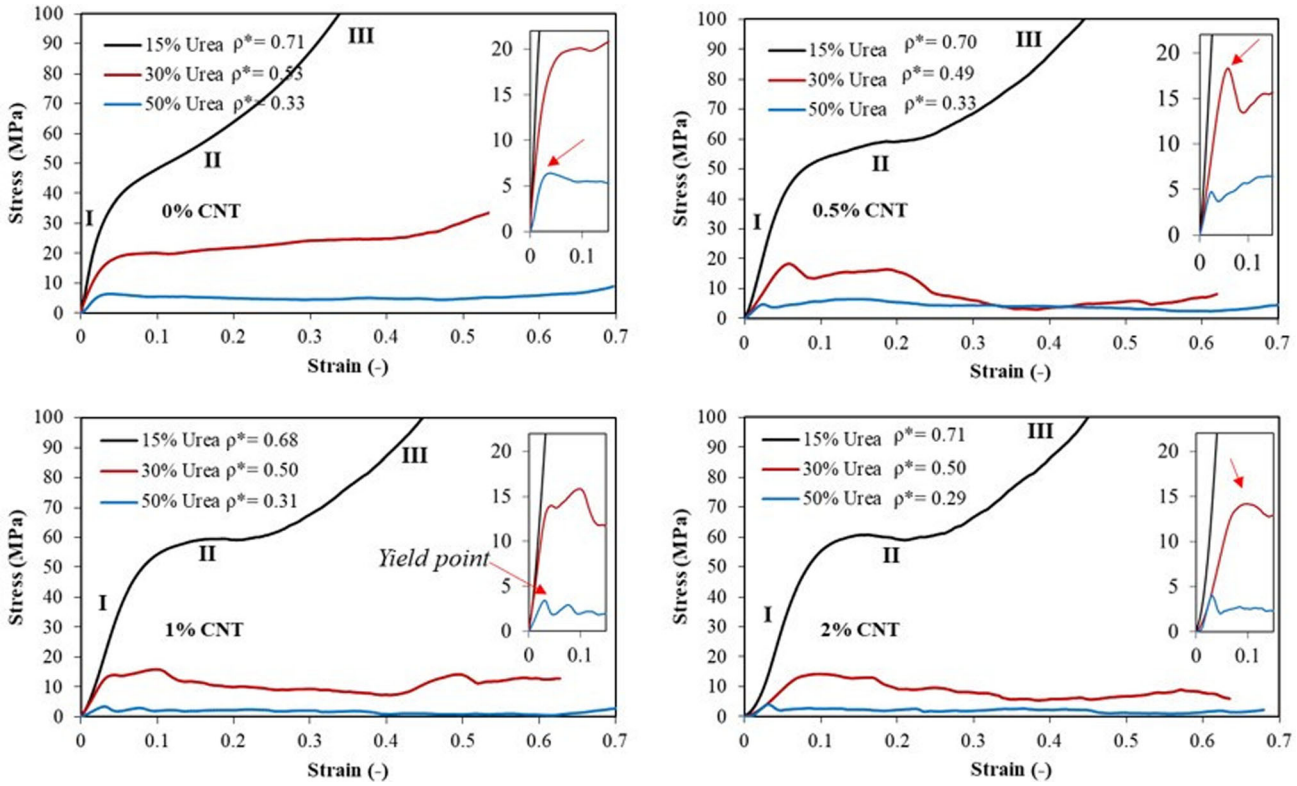

Fig. 11 Compressive stress–strain curves of the MWCNT/Al composite foams

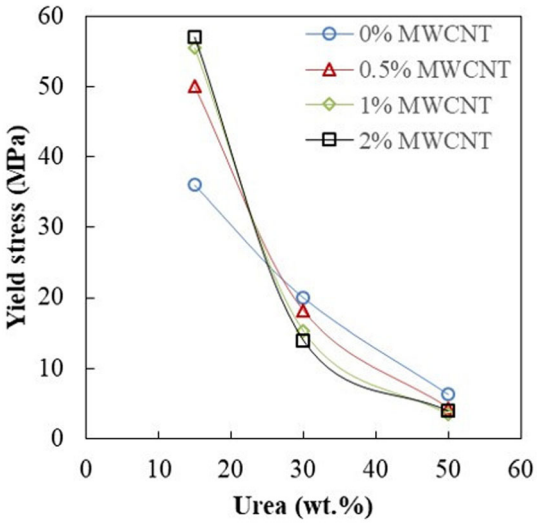

Fig. 12 Variation of yield stress with urea and MWCNT

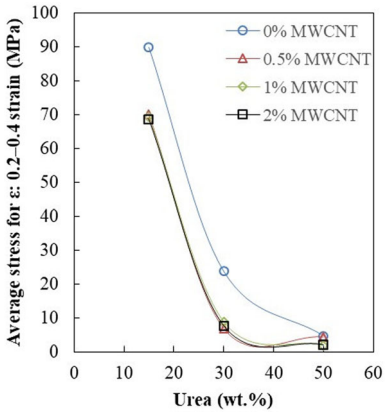

Fig. 13 Variation of average stress in the range of ε: 0.2–0.4 strain

density. An energy absorption value of 21.7 MJ/m^3 was obtained in pure aluminum foams with high relative density. On the other hand, this value decreased with the addition of MWCNT up to 2%. Energy absorption values for samples containing 0.5%, 1%, and 2% MWCNT were 15.22 MJ.m^{-3}, 15.53 MJ.m^{-3}, and 15.69 MJ.m^{-3}, respectively. Energy absorption values decreased by approximately 30%. An energy absorption value of 5.8 MJ m^{-3} was obtained in pure aluminum foams with medium relative density. With the addition of MWCNT, the energy absorption values of these samples decreased in a similar way as in the samples with high relative density. Samples containing 0.5%, 1%, and 2% MWCNT resulted in energy absorption values of 3.62 MJ m^{-3}, 3.28 MJ m^{-3} and 3.36 MJ m^{-3}, respectively. With the addition of MWCNT, the energy absorption value of the pure sample decreased more than 48%. The energy absorption value for pure aluminum foams with low relative density is

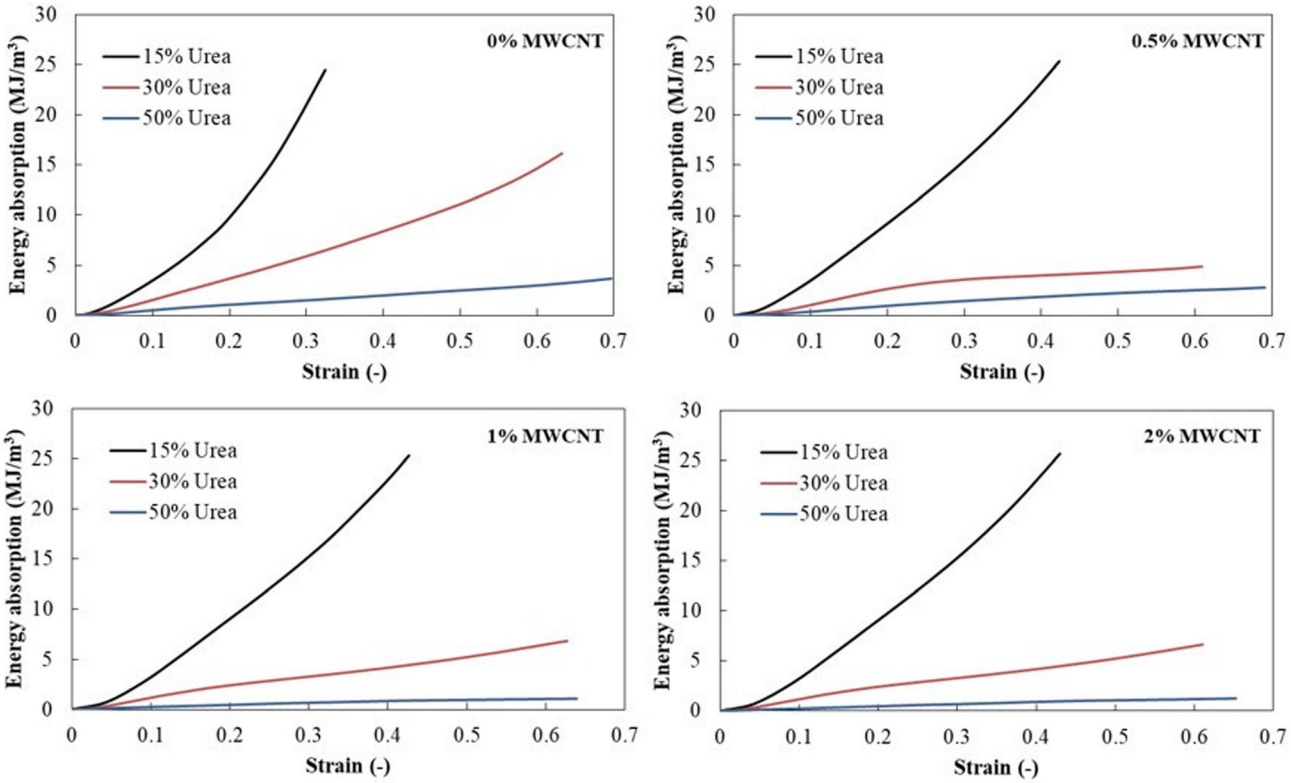

Fig. 14 Energy absorption curves of the MWCNT/Al composite foams

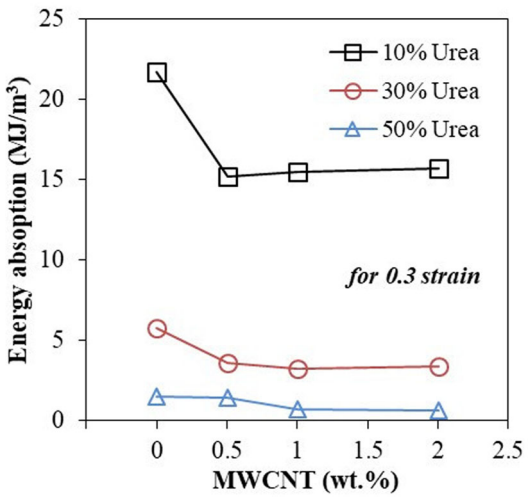

Fig. 15 Variation of energy absorption for ε: 0.3 strain

1.51 MJ m^{-3}. As in other samples, the addition of MWCNT decreased the energy absorption values in these samples. In samples containing 0.5%, 1%, and 2% MWCNT, the energy absorption values were 1.45 MJ m^{-3}, 0.68 MJ m^{-3} and 0.67 MJ m^{-3}, respectively. With the addition of 2% MWCNT, the energy absorption values of the pure aluminum foam decreased by approximately 56%.

4 Conclusions

In this study, MWCNT-reinforced (0%, 0.5%, 1%, and 2%) aluminum foams were produced with the powder metallurgy method. Spherical-shaped urea granules were used to form pores in the samples, and to obtain different amounts of porosity, the urea rates were determined as 15%, 30%, and 50%. Composite foams were produced by subjecting the mixtures (Al/MWCNT + Urea) obtained in the specified ratios to compression and sintering processes. Conclusions made from the results obtained from the tests conducted on the mechanical and physical properties of the produced samples have been summarized below.

- The porosity increased along with an increase in urea. The maximum average porosity was 69% in the samples produced with 50% urea.
- It was determined that MWCNT particles did not significantly affect porosity.
- The porosity structure of the produced samples was spherical in accordance with the urea granules used.
- It was found that the MWCNT particles were tubular and sometimes agglomerated in the cell wall.
- Density decreased due to the increase in porosity values and urea. The average minimum density value was determined as 0.84 g cm^{-3} in the samples produced with 50% urea.

- The hardness values of the foam sample cell walls increased with the increase in MWCNT ratio. The highest hardness value (65 HV) was determined in the foam samples containing 2% MWCNT produced with 15% urea.
- It was determined that the urea used as the pore-forming agent had a more considerable effect on crushing behavior than MWCNT particles used as reinforcing elements. However, the cell walls of the foams showed brittle fracture behavior with increasing MWCNT amount. The highest yield stress (57 MPa) was obtained in the 2% MWCNT-reinforced foam sample, and the highest average stress (89.9 MPa) for 0.2–0.4 strain was obtained in samples without MWCNT.
- The compression properties of the samples decreased with the decrease in the relative densities of the foams.

References

1. Muchhala D, Yadav B N, Kumar R, Mondal D P, Venkat A C,*Compos Part B* **176** (2019) 107304.
2. Wang J, Yang X, Zhang M, Li J, Shi C, Zhao N, Zou T, *Mater Lett* **161** (2015) 763.
3. Yang K, Yang X, Liu E, Shi C, Ma L, He C, Li Q, Li J, Zhao N, *Mater Sci Eng A* **690** (2017) 294
4. Yang K, Yang X, Liu E, Shi C, Ma L, He C, Li Q, Li J, Zhao N, *Mater Sci Eng A* **729** (2018) 487
5. Rajak D K, Kumaraswamidhas L A, Das S, *Ciência & Tecnologia dos Materiais* **29** (2017) 14.
6. Mu Y, Yao G, Liang L, Luo H, Zu G, *Scr Mater* **63** (2010) 629.
7. Kadkhodapour J, Raeisi S, *Comput Mater Sci* **83** (2014) 137.
8. Wang N, Maire E, Chen X, Adrien J, Li Y, Amani Y, Hu L, Cheng Y, *Mater Charact* **147** (2019) 11.
9. An Y, Yang S, Wu H, Zhao E, Wang Z, Mater Des 134 (2017) 44.
10. Badkul A, Saxena S, Mondal D P, *Compos Struct* **246**, (2020) 112419.
11. Duarte I, Ferreira J M, *Materials* **9** (2016) 79.
12. Yang X, Hu Q, Li W, Song H, Zou T, Zong R, Sha J, He C, Zhao N, *Fatigue Fract Eng Mater Struct* **43** (2020) 744.
13. Daoud A, *J Alloys Compd* **487** (2009) 618.
14. Smorygo O, Mikutski V, Marukovich A, Sadykov V, Bespalko Y, Stefan A, Pelin C E, *Compos Struct* **202** (2018) 917.
15. Fiedler T, Al-Sahlani K, Linul P A, Linul E, *J Alloys Compd* **813** (2020) 152181.
16. Zhang Q, Lin Y, Chi H, Chang J, Wu G, *Compos Struct* **183** (2018) 499.
17. Kumar N R, Rao N R, Gokhale A A, *Mater Sci Eng A* **598** (2014) 343.
18. Xu J, Yang X, He C, Yang K, Li W, Sha J, Zhao N, *J Mater Sci* **55** (2020) 7910.
19. Carvalho O, Buciumeanu M, Madeira S, Miranda G, Silva F S, *Compos Part B* **93** (2016) 229.
20. Han L, Li K, Sun J, Song Q, Wang Y, *Mater Sci Eng A* **735** (2018) 10.
21. Aldoshan A, Khanna S, *Mater Sci Eng A* **689** (2017) 17.
22. Yang K, Yang X, He C, Liu E, Shi C, Ma L, Li Q, Li J, Zhao N, *Mater Lett* **209** (2017) 68.
23. Yang X, Hu Q, Du J, Song H, Zou T, Sha J, He C, Zhao N, *Int J Fatigue* **121** (2019) 272.
24. Duarte I, Ventura E, Olhero S, Ferreira J M, *Carbon* **95** (2015) 589.
25. Zhang Z, Ding J, Xia X, Sun X, Song K, Zhao W, Liao B, *Mater Des* **88** (2015) 359.
26. Ogawa F, Yamamoto S, Masuda C, *Mater Sci Eng A* **711** (2018) 460.
27. Huang H, Fan G, Tan Z, Xiong D B, Guo Q, Guo C, Li Z, Zhang D, *Mater Sci Eng A* **699** (2017) 55.
28. Duarte I, Ventura E, Olhero S, Ferreira J M, *Mater Lett* **160** (2015) 162.
29. Duarte I, Ventura E, Olhero S, Ferreira J M F, *Ciência & Tecnologia dos Materiais* **28**, (2016) 5.
30. Yadav B N, Muchhala D, Sriram S, Mondal D P, *J Alloys Compd* **832** (2020) 154860.
31. Hassani A, Habibolahzadeh A, Bafti H, *Mater Des* **40**, (2012) 510.
32. Dahil L, Katirci R, Sümbül H I, *T Indian I Metals*, 73 (2020) 2739.
33. An J, Chen C, Zhang M, *Opt Laser Technol* **141** (2021) 107097.
34. Zhang M, Chen C, Huang Y, *Mater Sci Tech* **34** (2018) 968.
35. Zhao N Q, Jiang B, Du X W, Li J J, Shi C S, Zhao W X, *Mater Lett* **60**, (2006) 1665.
36. Jiang B, Zhao N Q, Shi C S, Li J J, *Scr Mater.* **53** (2005) 781.
37. Bakan H I, *Scr Mater* **55** (2006) 203.
38. Liu Z Y, Zhao K, Xiao B L, Wang W G, Ma Z Y, *Mater Des* **97** (2016) 424.
39. Zhang Z, Feng H, Xu T, Xin W, Ding J, Liu N, Wang Z, Wang Y, Xia X, Liu Y, *Compos Struct* **283** (2022) 115090.
40. Abhash A, Singh P, Kumar R, Pandey S, Sathaiah S, Shafeeq M M, Mondal D P, *Mater Sci Eng C* **109** (2020) 110600.
41. Markaki A E, Clyne T W, *Acta Mater* **49** (2001) 1677.
42. Gui M C, Wang D B, Wu J J, Yuan G J, Li C G, *Mater Sci Eng A* **286** (2000) 282.
43. Daoud A, *J Alloys Compd* **486** (2009) 597.
44. Zhang B, Lin Y, Li S, Zhai D, Wu G, *Compos Part B* **98** (2016) 288.
45. Jiang B, Wang Z, Zhao N, *Scr Mater* **56** (2007) 169.
46. Ashby M F, Evans T, Fleck N A, Hutchinson J, Wadley H, Gibson L, *Metal foams: a design guide*, Elsevier (2000).
47. Banhart J, *Prog Mater Sci* **46** (2001) 559.
48. Gibson L J, *Annu Rev Mater Sci* **30** (2000) 191.
49. Bafti H, Habibolahzadeh A, *Mater Des* **52** (2013) 404.
50. Chen B, Li S, Imai H, Jia L, Umeda J, Takahashi M, Kondoh K, *Compos Sci Technol* **113** (2015) 1.
51. Boesl B, Lahiri D, Behdad S, Agarwal A, *Carbon* **69** (2014) 79.
52. Yang D, Hu Z, Chen W, Lu J, Chen J, Wang H, Wang L, Jiang J, Ma A, *J Manuf Processes* **22** (2016) 290.